Macromolecules

ARTICLE

pubs.acs.org/Macromolecules

Unicore−Multicore Transition of the Micelle Formed by an Amphiphilic Alternating Copolymer in Aqueous Media by Changing Molecular Weight

Motoki Ueda, Akihito Hashidzume, and Takahiro Sato*

Department of Macromolecular Science, Graduate School of Science, Osaka University, 1-1 Machikaneyama-cho, Toyonaka, Osaka 560-0043, Japan

Supporting Information

ABSTRACT: Aggregates formed from amphiphilic alternating copolymer samples of sodium maleate and dodecyl vinyl ether (MAL/C12) of different molecular weights or (weight-average) degrees of polymerization N_{w1} (= 76−5000) were characterized by light scattering and fluorescence techniques in 0.05 M aqueous NaCl at pH 10 to investigate the molecular weight dependence of the micellar structure of amphiphilic polyelectrolytes. The light scattering and fluorescence data demonstrated a unicore−multicore transition of the MAL/C12 micelle at $N_{w1} \approx 300$. The structures of unicore and multicore micelles of MAL/C12 copolymers formed were analyzed using the flower micelle model and the flower necklace model, respectively. The data points for unicore micelles formed from the three low-molecular-weight MAL/C12 fractions were in good agreement with the flower micelle model of the minimum loop size determined by the rigidity of the polymer main chain, which we proposed previously [Kawata et al. Macromolecules 2007, 40, 1174−1180]. On the other hand, the data points for the four high-molecular-weight MAL/C12 fractions were nicely fitted to the flower necklace model, the conformation of which was represented as the touched bead model.

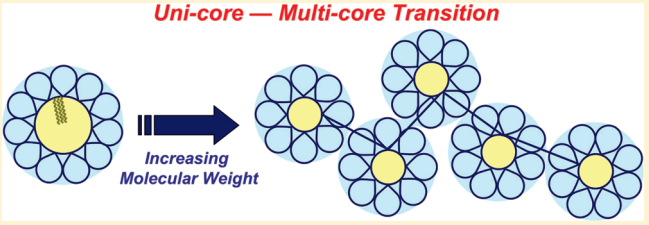

INTRODUCTION

Amphiphilic polyelectrolytes (APEs) comprise hydrophobic and ionizable monomer units. While hydrophobic monomer units tend to associate each other by strong hydrophobic attraction in aqueous media, charged monomer units repel each other as far as possible because of strong electrostatic repulsion. Thus, APEs exhibit various types of association behavior in aqueous media depending on the balance between hydrophobic attraction among hydrophobes and electrostatic repulsion among charges.[1] Their association behavior is of importance not only because they are useful as simple models for the formation of higher order structures of biological macromolecules but also because they are used in various fields of applications including cosmetics, drug delivery systems, paints, coatings, and personal care goods.[2] Therefore, the association behavior of APEs has been studied by a number of research groups in recent two or more decades. On the basis of these studies, the association behavior of APEs can be controlled by changing the chemical structure. However, the structure of micellar aggregates formed from APEs with random or alternating sequences in aqueous media had been unclear because of the complexity of the intramicellar electrostatic and hydrophobic interactions along the copolymer chains.

Recently, we have extensively investigated the structure of micelles formed from statistical vinyl copolymers bearing dodecyl groups as the hydrophobes, by static and dynamic light scattering combined with time-resolved fluorescence quenching measurements.[3] When the dodecyl content ranges from ca. 0.2 to 0.4 and the degree of polymerization is less than ca. 300, the APEs form unicore micelles in aqueous salt solution, and their hydrodynamic radii R_H were favorably compared with a flower micelle model of the minimum loop size determined by the copolymer chain stiffness (cf. Figure 8). More recently, it has been demonstrated that this flower micelle model is consistent with molecular dynamics simulation results for a dodecyl-carrying APE micelle with respect to the density distributions of dodecyl and ionic groups as well as main-chain carbons.[4]

From the analogy of spherical micelles formed by small molecular amphiphiles,[5] there may be an optimum aggregation number for dodecyl groups forming the hydrophobic core of the flower micelle. Therefore, if we increase the molecular weight or the degree of polymerization of a dodecyl-carrying APE at a fixed dodecyl content, we may expect a transition from the unicore to multicore micelle of the APE in aqueous media. Although some theoretical considerations on micelles of polysoaps with different degrees of polymerization[6] as well as a few reports on multicore micelle some amphiphilic copolymers[7] have been presented so far, to our best knowledge, there are no systematic studies on the molecular weight dependence of the

Received: November 24, 2010
Revised: February 25, 2011
Published: March 17, 2011

Scheme 1. Chemical Structure of the Copolymers Used in This Study

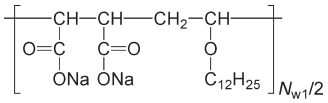

MAL/C12

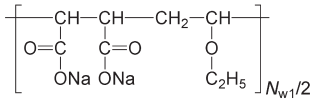

MAL/C2

micellar structure formed by APEs with random or alternating sequences at a fixed hydrophobic content.

High-molecular-weight APE samples are often used in various applications, so that the molecular weight dependence of the APE micellar structure is a basically important subject. In this study, we have chosen the alternating copolymer of sodium maleate and dodecyl vinyl ether (MAL/C12, Scheme 1) to study the molecular weight dependence of the micellar structure. The alternating copolymer has the fixed hydrophobic content and definite sequence distribution, so that we can study the molecular weight dependence without ambiguity from sequence heterogeneity. This type of alternating copolymer has been investigated by a number of research groups,[8−17] but the molecular weight dependency of the micellar structure remains unknown. In this study, we have prepared MAL/C12 copolymer samples of different molecular weights and characterized their micellar structure by light scattering and fluorescence techniques. The characterization data are indicative of the unicore−multicore transition of the MAL/C12 micelle at a certain molecular weight. Furthermore, we have analyzed the structure of the micelles formed from MAL/C12 copolymers by using the flower micelle model proposed previously[3] and a flower necklace model.

EXPERIMENTAL SECTION

Materials. Maleic anhydride (MAnh) was recrystallized from chloroform. Dodecyl vinyl ether (C12VE) and ethyl vinyl ether (C2VE) were distilled under reduced pressure and under atmospheric pressure, respectively. Tetrahydrofuran (THF) and benzene used for polymerization and hydrolysis were distilled over calcium hydride under ordinary pressure. Methanol used for light scattering was purified by distillation under atmospheric pressure. Water was purified by a Millipore Milli-Q system. NaCl was purified by recrystallization using water. Other reagents were used without further purification.

Preparation of the Polymers Used in This Study. Alternating copolymer samples of sodium maleate (MAL) and C12VE (MAL/C12) were prepared as follows: MAnh, C12VE, and 2,2′-azobis(isobutyronitrile) were placed in a flask equipped with a three-way stopcock and dried under vacuum for 1 h. The mixture was dissolved in THF, benzene, or a mixed solvent of THF/benzene, under an argon atmosphere at ambient temperature. The flask was immersed in an oil bath thermostated at 65 °C with stirring for 24 h. After polymerization, the reaction mixtures were poured into a large excess of methanol to precipitate the copolymer formed, and recovered samples were purified by reprecipitation from THF into methanol twice. Seven copolymer samples obtained were then divided into 37 fractions by successive fractional precipitation using acetone and methanol as the solvent and precipitant, respectively, and seven fractions were selected for the following measurements. Ratios of the weight to number-average molecular weight M_{w1}/M_{n1} of the selected fractions were determined by size exclusion chromatography (SEC) using a calibration curve constructed by standard polystyrene samples (cf. the fourth column of Table 1). The ratios ranged from 1.3 to 1.8, indicating relatively low fractionation efficiency of the copolymer, but we did not make further fraction to maintain amounts of the fractions.

Table 1. Molecular Characteristics of MAL/C12 Copolymer Fractions Used in This Study

fraction code	$M_{w1}/10^4$	$N_{w1}/10^2$ [c]	M_{w1}/M_{n1} [d]	M_{z1}/M_{w1} [a]
MAL/C12-1	1.2[a]	0.76	1.6	1.3
MAL/C12-2	1.6[a]	0.95	1.5	1.5
MAL/C12-3	3.4[a]	2.0	1.8	—[e]
MAL/C12-4	7.3[b]	4.5	1.3	
MAL/C12-5	27[b]	16	1.4	
MAL/C12-6	70[b]	43	1.7	
MAL/C12-7	83[b]	50	1.7	

[a] Determined by sedimentation equilibrium measurements in methanol containing 0.10 M $LiClO_4$ with the specific density increment $\partial\rho/\partial c$ = 0.459 and the specific refractive index increment $\partial n/\partial c$ = 0.135 cm^3/g (at 675 nm) for dialyzed solutions of MAL/C12 at 25 °C. [b] Determined by SLS measurements in methanol containing 0.10 M $LiClO_4$ with $\partial n/\partial c$ = 0.128 cm^3/g (at 532 nm). [c] The weight-average degree of polymerization (the sum of MAL and C12 units) (= $M_{w1}/\overline{M}_0$ with $\overline{M}_0$ = 164).[18] [d] Estimated by SEC for the corresponding parent copolymers of MAnh and DVE using THF as eluent. [e] Not determined.

The MAnh moieties of the selected fractions were then hydrolyzed with 1.0 M aqueous NaOH in THF under an argon atmosphere at ambient temperature to obtain MAL/C12 fractions. The MAL/C12 fractions were purified by dialysis against water for 4 days, neutralized by adding aqueous NaOH, and then recovered by freeze-drying. Weight-average molecular weights M_{w1} of the MAL/C12 fractions were determined by sedimentation equilibrium or static light scattering (SLS) (cf. Supporting Information).[3,18] As listed in Table 1, M_{w1} of the MAL/C12 fractions cover a wide molecular weight range.

Alternating copolymer samples of MAL and C2VE (MAL/C2, Scheme 1) were prepared in the same manner as described above. For the fractionation procedure, however, THF and diethyl ether were employed as the solvent and precipitant, respectively. Ratios M_{w1}/M_{n1} of the fractions of MAL/C2 obtained ranged from 1.2 to 1.8. Molecular weights of the fractions were determined in 0.05 M aqueous NaCl at 25.0 °C by SLS with $\partial n/\partial c$ = 0.197 cm^3/g (at 532 nm) (see below).

Measurements. *a. Preparation of 0.05 M aqueous NaCl Solutions for Measurements.* Solutions for the following measurements were prepared according to the procedure reported previously.[3,19] Each freeze-dry copolymer fraction (the sodium salt form) was dissolved in pure water at room temperature and heated at 90 °C for 15 min. The solution pH was adjusted to 10 by adding a small amount of 0.10 M aqueous NaOH. The solution was then mixed with 0.10 M aqueous NaCl of the same pH by 1:1 volume ratio and stirred overnight. This original solution was diluted with 0.05 M aqueous NaCl of the same pH to prepare test solutions of different concentrations.

b. Light Scattering. Simultaneous static and dynamic light scattering (SLS and DLS, respectively) experiments were performed for 0.05 M aqueous NaCl solutions (pH = 10) of MAL/C12 fractions as well as MAL/C2 fractions at 25.0 °C using an ALV/SLS/DLS-5000 light scattering instrument equipped with an ALV-5000 multiple τ digital correlator using a Nd:YAG (532 nm) laser. The excess Rayleigh ratio R_θ obtained by SLS and the first cumulant Γ obtained by DLS (with the CONTIN analysis[20,21]) for each solution were analyzed using the

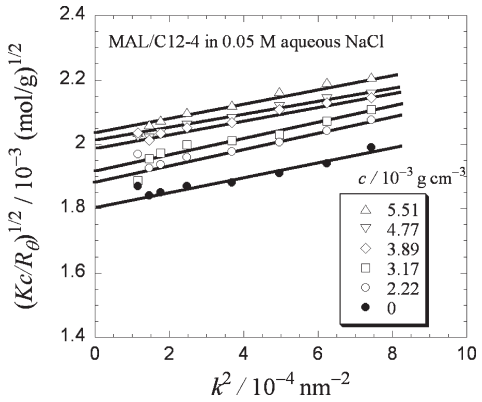

Figure 1. Angular dependences of $(Kc/R_\theta)^{1/2}$ for fraction MAL/C12-4 in 0.05 M aqueous NaCl at different polymer concentrations c.

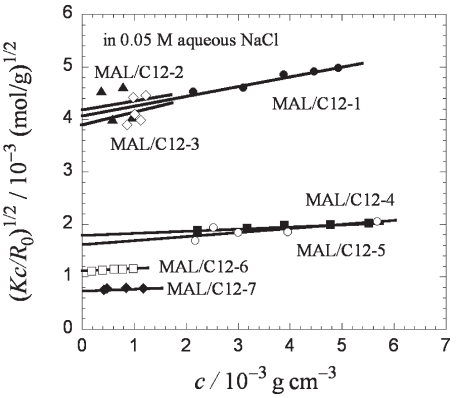

Figure 2. Concentration dependences of $(Kc/R_0)^{1/2}$ for all the MAL/C12 fractions investigated in 0.05 M aqueous NaCl.

following standard equations:[3,20,21]

$$\lim_{k \to 0} (Kc/R_\theta)^{1/2} \equiv (Kc/R_0)^{1/2} = {M_w}^{-1/2} + A_2 {M_w}^{1/2} c + O(c^2) \quad (1a)$$

$$\lim_{c \to 0} (Kc/R_\theta)^{1/2} = {M_w}^{-1/2}\left[1 + \frac{1}{6}\langle S^2\rangle k^2 + O(k^4)\right] \quad (1b)$$

$$\lim_{k,c \to 0} \Gamma/k^2 = k_B T/6\pi\eta_0 R_H \quad (1c)$$

to determine the weight-average molar mass M_w, the second virial coefficient A_2, the z-average square radius of gyration $\langle S^2\rangle_z$, and the hydrodynamic radius R_H of the micelle in the solution. Here, K is the optical constant, c is the copolymer mass concentration, k^2 is the square of the scattering vector, $k_B T$ is the Boltzmann constant multiplied by the absolute temperature, and η_0 is the solvent viscosity coefficient. Values of the specific refractive index increments $\partial n/\partial c$ at 532 nm for dialyzed 0.05 M aqueous NaCl solutions of MAL/C12 and MAL/C2, necessary to calculate K, were measured to be 0.145 and 0.197 cm^3/g, respectively.

For some MAL/C12 fractions in 0.05 M aqueous NaCl, DLS data showed bimodal relaxations, which indicate that the solutions contain two scattering components with largely different sizes. In such cases, the scattering intensity of the major fast relaxation component in each solution was extracted from the total scattering intensity using the relaxation spectrum obtained by DLS and analyzed to determine the weight-average molar mass M_w and the hydrodynamic radius R_H of the major component, as in the previous study.[20,21]

c. Fluorescence. A small amount of a concentrated methanol solution of pyrene was added to an aqueous solution of MAL/C12 (pH 10) prepared as described above, and the solution was stirred overnight. The solution was then mixed with 0.1 M aqueous NaCl of pH 10 (1/1, v/v) and stirred overnight, followed by filtration with a 0.2 μm PTFE membrane filter. After the solution was purged with argon for ca. 30 min, steady-state fluorescence spectrum and fluorescence decay profile $I(t)$ of the solution were recorded on an F-4500 fluorescence spectrometer (Hitachi) and a NAES 550 system (Horiba) equipped with a flash lamp filled with hydrogen, respectively, in the same manners as the previous.[3,4,20]

The fluorescence decay profiles were analyzed by the Infelta−Tachiya equation[20,22−25]

$$\ln\left[\frac{I(t)}{I(0)}\right] = -\left(k_0 + \frac{k_E k_-}{k_E + k_-}\bar{n}\right)t - \left(\frac{k_E}{k_E + k_-}\right)^2 \bar{n}\left[1 - e^{-(k_E + k_-)t}\right] \quad (2)$$

where k_0 is the fluorescence decay rate constant for an excited free pyrene, k_E and k_- are the rate constants for the excimer formation in a micelle containing two pyrene molecules and for exit of a free pyrene molecule from the micelle, respectively, and $\bar{n}$ is the average number of pyrene molecules in a micelle. Those parameters in eq 2 were determined by the curve fitting to experimental $I(t)$, and the number of hydrophobic cores per micelle n_c was calculated by[3,4,20]

$$n_c = \frac{[\mathrm{Py}]M_w}{1000 c N_A \bar{n}} \quad (3)$$

with $\bar{n}$ determined. Here, [Py] is the molar concentration of pyrene measured by absorption spectroscopy, M_w is the molar mass of the micelle measured by SLS (see above), and N_A is the Avogadro constant.

RESULTS AND DISCUSSION

Characterization of MAL/C12 Copolymer Aggregates in 0.05 M Aqueous NaCl. Figure 1 shows the SLS result of fraction MAL/C12-4 in 0.05 M aqueous NaCl. By extrapolation to the zero k, we obtained $(Kc/R_0)^{1/2}$ at zero scattering angle at finite concentrations, and the results of $(Kc/R_0)^{1/2}$ such obtained are plotted against c for all the MAL/C12 fractions investigated in Figure 2. From the intercept and slope of the plot, we determined the weight-average molar mass M_w (or the weight-average number of monomer units N_w per aggregate) and the second virial coefficient A_2 for each fraction (cf. eq 1a). Since data points for fractions MAL/C12-2 and -3 were scattered, we extrapolated the plots to the zero c by assuming that A_2 of the fractions are similar to that of fraction MAL/C12-1. For the four high molecular weight fractions, z-average square radii of gyration $\langle S^2\rangle_z$ were also estimated from the slope and intercept of the plot of $(Kc/R_\theta)^{1/2}$ vs k^2 at $c = 0$, as shown by filled circles in Figure 1 (cf. eq 1b).

Results of DLS for MAL/C12 fractions in 0.05 M aqueous NaCl are shown in Figure 3, where Γ is the first cumulant. By extrapolation to the zero c, we determined the diffusion coefficient and converted to the hydrodynamic radius R_H using the Einstein−Stokes equation. Table 2 lists all SLS and DLS results for Mal/C12 fractions in 0.05 M aqueous NaCl. For most of fractions, N_w in Table 2 is larger than N_{w1} in Table 1: the weight-average aggregation number m_w (= N_w/N_{w1}) ranges from 1 to 4.5 (Table 2). On the other hand, A_2 of the MAL/C12 aggregates are positive, indicating that the aggregates little dissociate by dilution. (Values of A_2 seem to be slightly smaller than those expected for polyelectrolytes, which may come from partial cancellation of the electrostatic interaction by the hydrophobic

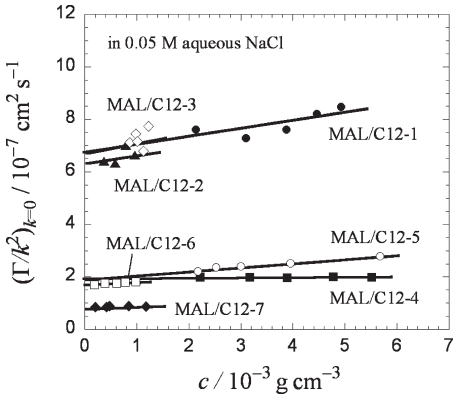

Figure 3. Concentration dependences of $(\Gamma/k^2)_{k=0}$ for all the MAL/C12 fractions investigated in 0.05 M aqueous NaCl.

Table 2. Characteristics of Major Aggregating Components of MAL/C12 Copolymer Fractions in 0.05 M Aqueous NaCl at pH 10

fraction code	$M_w/10^4$	$N_w/10^2$ [a]	m_w [b]	A_2 [c]	$\langle S^2\rangle_z^{1/2}$/nm	R_H/nm	ρ [d]
MAL/C12-1	6.1	3.3	4.5	6.3		3.7	
MAL/C12-2	5.7	3.1	3.1			3.8	
MAL/C12-3	6.6	3.5	1.7			3.7	
MAL/C12-4	31	17	3.7	0.81	27	12	2.2
MAL/C12-5	38	20	1.3	1.8	19	12	1.6
MAL/C12-6	81	44	1.0	0.57	26	15	1.7
MAL/C12-7	170	94	1.8	2.0	52	26	1.9

[a] Weight-average monomer-unit number per aggregate (= $M_w/\overline{M}_0$ with $\overline{M}_0$ = 168). [b] Weight-average aggregation number (= M_w/M_{w1}). [c] Second virial coefficient in units of 10^{-4} cm^3 mol/g^2. [d] Ratio of $\langle S^2\rangle_z^{1/2}$ to R_H.

interaction of C12.) Ratios ρ of $\langle S^2\rangle_z^{1/2}$ to R_H are slightly larger than those expected for random coils (1.3−1.5) as well as spheres (0.78). This may be due to dispersities in the molecular weight and aggregation number[26] because the dispersity increases $\langle S^2\rangle_z^{1/2}$ more than R_H.

Figure 4a demonstrates steady-state fluorescence spectra of pyrene solubilized in 0.05 M aqueous NaCl solutions of MAL/C12-1 fraction. The ratio I_3/I_1 of the intensities of the third (383 nm) to the first (372 nm) vibronic peaks for the pyrene solubilized is ca. 0.9, which is much larger than the I_3/I_1 value in the bulk water phase (ca. 0.6)[27] and comparable to that (= 0.96) in aqueous micellar solution of sodium dodecyl sulfate.[28] Furthermore, the concentration [Py] of pyrene solubilized in the copolymer solution considerably exceeds the upper limit of the solubility of pyrene in water (<1 μM). These observations are indicative of the formation of hydrophobic microdomains in the aqueous MAL/C12 copolymer solutions. It should be noted here that the fluorescence spectra exhibits a broad band around 480 nm due to pyrene excimer at higher [Py], indicating that plural pyrene molecules are incorporated into a hydrophobic microdomain.

Figure 4b shows decay profiles of the fluorescence intensity $I(t)$ around 400 nm from pyrene solubilized in the solution of MAL/C12-1 fraction in 0.05 M NaCl after excitation of pyrene by a 337 nm light pulse of negligible duration at t = 0. Whereas $I(t)$ decays single-exponentially with the lifetime of excited pyrene monomer at a lower [Py] (= 1.1 μM), it exhibits a faster decay component at higher [Py]. This faster decay corresponds

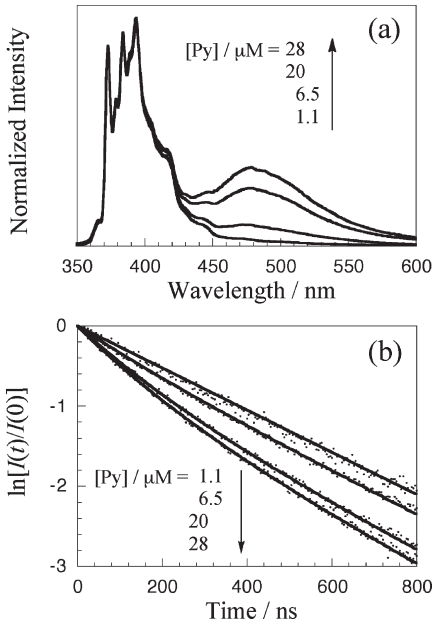

Figure 4. Steady-state fluorescence spectra for pyrene solubilized in 0.05 M NaCl solutions of MAL/C12-1 ($c = 5 \times 10^{-3}$ g/cm^3) (a) and fluorescence decay profiles around 400 nm for the solutions shown in panel a (b); curves in panel b, fitting results calculated by the Infelta−Tachiya kinetics (cf. eq 2).[22−25]

Table 3. Parameters Obtained from the Fluorescence Decay Experiments for MAL/C12 Copolymer Fractions in 0.05 M NaCl at pH 10

fraction code	[Py]/μM	$k_0/\mu s^{-1}$	$k_E/\mu s^{-1}$	$k_-/\mu s^{-1}$	$\bar{n}$	n_c
MAL/C12-1	6.5	2.6	3.1	0.10	0.29	1.2
MAL/C12-1	20	2.6	3.0	0.14	0.75	1.4
MAL/C12-1	28	2.6	2.9	0.20	0.93	1.6
MAL/C12-2	13	2.7	5.4	0.54	0.80	0.84
MAL/C12-2	20	2.7	5.3	0.59	0.96	1.1
MAL/C12-3	10	2.5	3.3	0.10	0.38	0.95
MAL/C12-3	24	2.5	3.1	0.10	0.80	1.1
MAL/C12-3	33	2.5	3.1	0.13	1.0	1.1
MAL/C12-4	24	2.5	4.9	0.59	0.70	16
MAL/C12-4	34	2.5	5.0	0.84	0.99	16
MAL/C12-5	22	2.6	3.0	0.20	0.39	27
MAL/C12-6	16	2.6	4.1	0.10	0.25	45
MAL/C12-6	31	2.6	4.1	0.37	0.45	49
MAL/C12-7	14	2.5	3.0	0.10	0.19	110
MAL/C12-7	30	2.5	3.0	0.20	0.41	110

to the quenching of fluorescence due to pyrene monomer by excimer formation within a hydrophobic microdomain (cf. Figure 4a), which returns to the ground-state emitting light around 480 nm being out of the experimental window.

These fluorescence decay profiles were analyzed on the basis of the Infelta−Tachiya kinetics (eq 2). As can be seen in Figure 4b, solid curves demonstrate satisfactory fits for the experimental $I(t)$. Fluorescence decay profiles for all the MAL/C12 fractions were also analyzed in the same manner to determine the kinetic parameters, as listed in Table 3. The decay rate constant k_0 of excited pyrene as well as the rate constants k_E for the excimer formation and k_- for exit of

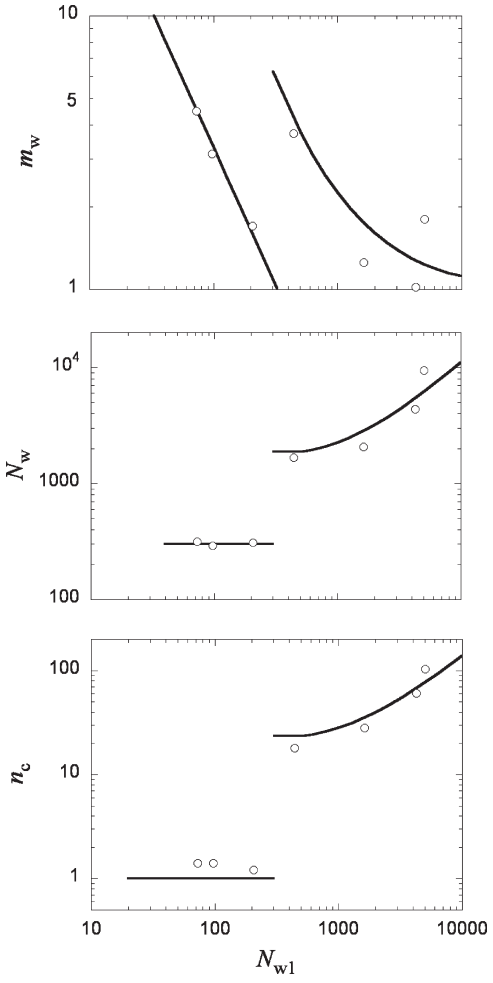

Figure 5. Degree of polymerization N_{w1} dependences of the aggregation number m_w (top), the number of monomer units N_w per micelle (middle), and the hydrophobic core number n_c per micelle (bottom) for MAL/C12 copolymer fractions in 0.05 M aqueous NaCl.

pyrene from the microdomain are essentially independent of the polymer molecular weight M_{w1}. As shown in the last column of Table 3, numbers of hydrophobic cores per micelle n_c calculated by eq 3 are about unity for the three low-molecular-weight MAL/C12 fractions, but it remarkably increases for the four high-molecular-weight fractions. These results demonstrate that MAL/C12 forms unicore micelles at $N_{w1} \lesssim 300$ but multicore micelles at $N_{w1} \gtrsim 300$ in 0.05 M aqueous NaCl.

Unicore−Multicore Transition of the MAL/C12 Copolymer Micelle. Figure 5 summarizes the degree of polymerization N_{w1} dependences of the aggregation number m_w, the hydrophobic core number n_c, and the number of monomer units per micelle N_w. In the unicore region ($N_{w1} \lesssim 300$), m_w is inversely proportional to and N_w is independent of N_{w1}. Thus, we can say that the unicore micelle of the MAL/C12 copolymer consists of a fixed monomer unit number $N^* \approx 300$.

On the other hand, in the multicore region ($N_{w1} \gtrsim 300$), m_w seems to decrease and tend to unity with increasing N_{w1}, which may be approximately fitted to the empirical equation

$$m_w = 1 + \frac{1160}{N_{w1}} \qquad (4)$$

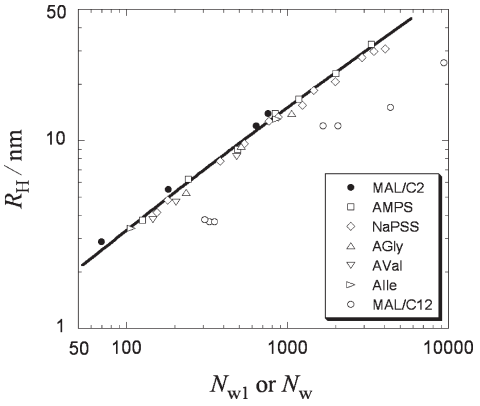

Figure 6. Plots of R_H against N_{w1} or N_w for MAL/C2 copolymers (●), AMPS homopolymers (□),[29] NaPSS homopolymers (◇),[30] AGly homopolymers (△),[3] AVal homopolymers (▽),[3] AIle homopolymers (tilted △),[3] and MAL/C12 copolymers (○) in 0.05 M aqueous NaCl.

Scheme 2. Chemical Structures of AMPS/C12, AXaa/C12, and A/C12 Copolymers

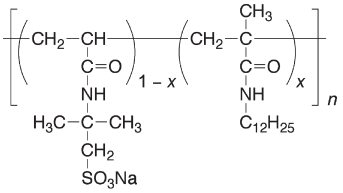

AMPS/C12

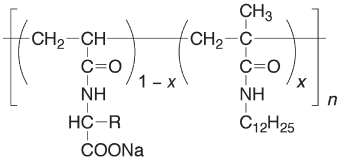

AXaa/C12

AGly/C12 (R = H)
AVal/C12 (R = $CH(CH_3)_2$)
AIle/C12 (R = $CH(CH_3)CH_2CH_3$)

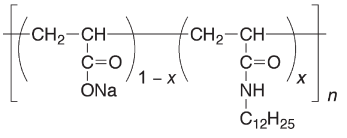

A/C12

(the solid curve at $N_{w1} > 300$ of the top panel of Figure 5). As mentioned above, A_2 data indicate that the micelle does not dissociate by dilution within the concentration ranges investigated, and thus the critical aggregation concentration should be very low for the copolymer. At present, we have no molecular interpretation for eq 4. Using eq 4, we may calculate N_w and n_c by

$$N_w = m_w N_{w1}, \quad n_c = m_w N_{w1}/N_c \qquad (5)$$

where N_c is the number of monomer units per hydrophobic core. The solid curves at $N_{w1} > 300$ of the middle and bottom panels of Figure 5 indicate are drawn using eqs 4 and 5 with $N_c = 82$. It is

dx.doi.org/10.1021/ma102635y |*Macromolecules* 2011, 44, 2970–2977

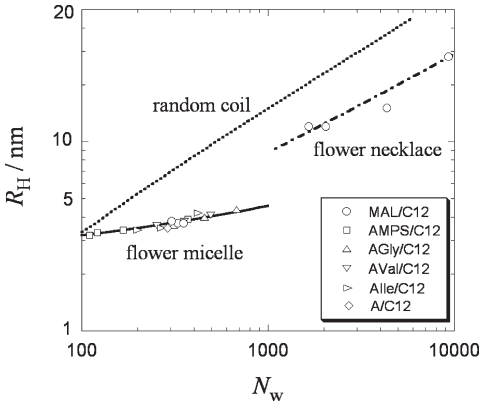

Figure 7. Plots of R_H against N_w for MAL/C12 copolymers (○) as well as AMPS/C12 copolymers (□),[3] AGly/C12 copolyemrs (△),[3] AVal/C12 copolymers (▽),[3] Alle/C12 copolymers (tilted △),[3] and A/C12 copolymers (◇)[4] in 0.05 M aqueous NaCl. The dotted line represents R_H values for MAL/C2 copolymers in 0.05 M NaCl. The solid and broken lines represent R_H estimated based on the unicore flower micelle model of the minimum loop size and on the flower necklace model consisting of linearly connected flower micelles with the minimum loop size, respectively.

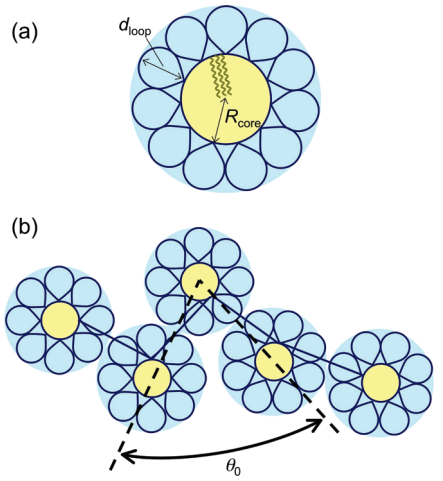

Figure 8. Schematic representations of the flower micelle model of the minimum loop size (a), where only a part of hydrophobic chains are drawn and those attached to the loops outside the hydrophobic core are omitted for simplicity, and the flower necklace model consisting of linearly connected flower micelles with the minimum loop size (b), where hydrophobic chains are omitted for simplicity.

noted that $N_c < N^*$; i.e., the unit core size in the multicore micelle is smaller than the core size of the unicore micelle.

All the quantities m_w, N_w, and n_c are discontinuous at $N_{w1} = N^*$. The average copolymer concentration inside the micelle, calculated by $3M_w/4\pi R_H{}^3 N_A$, also suddenly changes from 0.37 ± 0.5 g/cm^3 to less than 0.1 g/cm^3 at $N_{w1} = N^*$. We refer to this discontinuity as the unicore−multicore transition of the MAL/C12 micelle. To the best of our knowledge, this is the first demonstration of the transition by changing the molecular weight of the amphiphilic copolymer.

Micellar Structures. Figure 6 compares the degree of polymerization N_{w1} dependence of the hydrodynamic radius R_H for MAL/C2 (filled circles) with the N_w dependence of R_H for MAL/C12 (unfilled circles) in 0.05 M aqueous NaCl. The MAL/C2 copolymer may take a random coiled conformation because the hydrophobic interaction among ethyl groups on C2VE units is not strong in aqueous solution. In fact, the data points for MAL/C2 are close to those for homopolymers of sodium 2-acrylamido-2-methylpropanesulfonate (AMPS)[29] and of sodium salt of *N*-acryloyl-amino acids (AGly, AVal, AIle)[3] (Scheme 2 where $x = 0$) as well as sodium poly(styrenesulfonate) (NaPSS)[30] in 0.05 M aqueous NaCl. All those data points are almost fitted to the theoretical line (the solid line in Figure 6) calculated by the theory of Yamakawa et al.,[31] for wormlike touched bead model with the persistence length q = 3.0 nm, the bead diameter d_b = 1.5 nm, the molar mass per unit contour length M_L = 900 nm^{-1}, and the excluded volume strength B = 15 nm.

On the other hand, the data points for the MAL/C12 copolymer appreciably deviate downward from those for the randomly coiled polyelectrolytes. As mentioned above, MAL/C12 forms micelles due to the strong hydrophobic interaction among dodecyl groups. Figure 6 indicates that both unicore and multicore micelles of MAL/C12 take more compact conformations than do the randomly coiled polyelectrolytes.

So far, we have studied the unicore micelle structure formed by several amphiphilic statistical vinyl copolymers possessing dodecyl groups as the hydrophobic moiety, as shown in Scheme 2.[3,4,32] Figure 7 collects R_H data for the unicore micelles of those copolymers in 0.05 M aqueous NaCl. It is noted that N_{w1} of all the previous random copolymer samples shown in the figure are less than 300 (and $x \leq 0.4$). As already demonstrated, R_H data for the unicore micelles of those random copolymers are consistent with the flower micelle model of the minimum loop size, as schematically shown in Figure 8a. In this model, the loop size is determined by the stiffness of the copolymer chain expressed in terms of the persistence length q, and the radius R_{core} of the hydrophobic core and the dimension d_{loop} of the minimum loop are calculated by[3,4]

$$\frac{4\pi}{3} R_{core}{}^3 = \lambda \left(\frac{N_w l}{1.6q} + 1 \right) v_{C12}, \quad d_{loop} = 0.62q \qquad (6)$$

where l is the contour length per monomer unit (= 0.25 nm), v_{C12} denotes the molecular volume of dodecyl group (= 0.35 nm^3), and $1.6q$ is the contour length of the minimum loop. We assumed that λ dodecyl groups are included in the core at each root of the loop. Choosing q = 3 nm (the value used to calculate the theoretical curve in Figure 6) and λ = 4.5, the hydrodynamic radius R_H as the sum of R_{core} and d_{loop} calculated by eq 6 fits the experimental results for the amphiphilic random copolymers as shown by the solid line in Figure 7. It is noted that the minimum loop consists of 19 monomer units, and only 25% of dodecyl groups are inside the hydrophobic core.

The results for MAL/C12 shown in Figure 6 are replotted in Figure 7 by unfilled circles. The data points for the three low-molecular-weight MAL/C12 fractions are nicely fitted to the solid line of the flower micelle model of the minimum loop size, but the data points for the four high molecular weight fractions deviate upward from the solid line.

The spherical micelle formed by small molecular amphiphiles is known to have some optimum aggregation number. Similarly, micelles formed by polymeric amphiphiles should also have an optimum aggregation number of hydrophobes, which is proportional to the optimum aggregation number N^* of monomer units. The constant N_w in the unicore region ($N_{w1} \lesssim 300$) shown in Figure 5 corresponds to this optimum aggregation number of monomer units, which leads to the inversely proportionality of m_w to N_{w1} from eq 5.[33]

dx.doi.org/10.1021/ma102635y |*Macromolecules* 2011, 44, 2970–2977

When the number of monomer units of the single copolymer chain exceeds this optimum aggregation number N^*, the chain may not be able to form stable unicore flower micelle but tends to form a multicore flower micelle by aggregating with other copolymer chains. Previously, Borisov and Helperin[6] theoretically considered the flower necklace model, where n_c unit flower micelles, each of which comprises N_c monomer units, are connected linearly by bridge chains (see Figure 8b). From the results shown in Figure 5, N_c should be taken to be 82 and n_c be calculated by eq 5, if we apply this model to the multicore micelles of the MAL/C12 copolymer.

The conformation of this model may be represented as the touched bead model with the bond length (= bead diameter) d_n and the bond angle θ taking from 60° to 180° without steric hindrance between the second nearest neighboring unit flower micelles. (This touched bead model should be distinguished from the wormlike touched bead model for the homopolyelectrolyte and MAL/C2 copolymer chains used in Figure 6.) The bead diameter d_n of the present touched bead model is identical with the diameter of the unit flower micelle, which may be estimated from $2(R_{core} + d_{loop})$ (= 6.2 nm) where R_{core} and d_{loop} are calculated from eq 6 with $N_w = N_c = 82$ and $q = 3$ nm. On the other hand, its persistence length q_n may be given by

$$q_n = \frac{d_n}{2}\left(\frac{3 - \cos 60^\circ}{1 + \cos 60^\circ}\right) + \frac{1}{4\kappa^2 Q} \qquad (7)$$

On the right-hand side of the equation, the first term is the intrinsic persistence length of the touched bead model derived from its characteristic ratio,[34,35] and the second term represents the electrostatic one[36,37] calculated from the Debye screening length κ^{-1} and the Bjerrum length Q. In 0.05 M aqueous NaCl, the second term (= 0.66 nm) is much smaller than the first one (= 5.2 nm). Furthermore, the excluded volume effect on this touched bead model[29−31] is characterized by the excluded volume strength B_n, which is taken as an adjustable parameter.

Using the above parameters, we can calculate R_H for the flower necklace model according to Yamakawa et al.'s theory.[31] When the only adjustable parameter B_n is chosen to be 2 nm, we obtain the dot-dash line in Figure 7, which fits to the experimental data for the multicore micelle of the MAL/C12 copolymer.

Borisov and Helperin[6] also suggested the possibility of branched structures for the multicore micelle. As the simplest branched architecture, we consider the three-arms regular star, of which R_H in a good solvent diminishes from that of the linear structure by the factor $g_H = 0.96$.[38] A similar good fit was obtained for the four-arm regular star architecture if B_n was selected to be 4.8 nm. However, R_H for the randomly branched chain of the functionality 3 in the unperturbed state[39] was too small to fit the experimental data for the multicore micelles ($g_H = 0.09−0.12$). Therefore, we can exclude the possibility of the randomly branched architecture for the multicore micelle of the MAL/C12 copolymer, but not the possibility of a branch architecture with a few branch points.

CONCLUSION

Aggregates formed from MAL/C12 alternating copolymers of different weight-average degrees of polymerization N_{w1} (= 76−5000) were characterized by light scattering and fluorescence techniques in 0.05 M aqueous NaCl at pH 10 to investigated the N_{w1} dependence of the micellar structure of amphiphilic polyelectrolytes. The light scattering and fluorescence data demonstrated that MAL/C12 formed unicore micelles at $N_{w1} \lesssim 300$ but multicore micelles at $N_{w1} \gtrsim 300$ in 0.05 M aqueous NaCl. In the unicore region ($N_{w1} \lesssim 300$), the weight-average aggregation number m_w (= M_w/M_{w1}) was inversely proportional to and the number of monomer units per micelle N_w was 300 independent of N_{w1}, indicating that the unicore micelle of the MAL/C12 copolymer consists of a fixed monomer unit number $N^* \approx 300$. On the other hand, in the multicore region ($N_{w1} \gtrsim 300$), m_w seemed to decrease and tend to unity with increasing N_{w1}, whereas N_w and the number of hydrophobic cores per micelle n_c increased with increasing N_{w1}, where the number of monomer units per hydrophobic core N_c was 82. All the quantities m_w, N_w, and n_c are discontinuous at $N_{w1} = N^*$, indicative of the unicore−multicore transition of the MAL/C12 micelle.

The structures of unicore and multicore micelles of MAL/C12 copolymers were analyzed using the flower micelle model and the flower necklace model, respectively. The data points for unicore micelles formed from the three low-molecular-weight MAL/C12 fractions were in good agreement with the flower micelle model of the minimum loop size determined by the rigidity of the polymer main chain, which we proposed previously. On the other hand, the data points for the four high-molecular-weight MAL/C12 fractions deviated upward from the flower micelle model but were nicely fitted to the flower necklace model, the conformation of which was represented as the touched bead model consisting of n_c unit flower micelles of $N_c = 82$, when the only adjustable parameter, i.e., the excluded volume strength B_n, is chosen to be 2 nm. A branched architecture with a few branch points also provided a good agreement for the multicore micelles, but the randomly branched chain did not. We are going to study the micellar structure of the copolymer by small-angle X-ray scattering.

Various micellar solution properties may drastically change by the unicore−multicore transition in amphiphilic polyelectrolytes (APE). Thus, the understanding of the transition must be important in applications of APE in various fields, and it is an important task to establish the interrelation between the micellar structural transition and solution properties.

ASSOCIATED CONTENT

Supporting Information. Determination of molecular weights of all MAL/C12 copolymer fractions by sedimentation equilibrium and light scattering. This material is available free of charge via the Internet at http://pubs.acs.org.

AUTHOR INFORMATION

Corresponding Author

*Fax +81-6-6850-5461; e-mail tsato@chem.sci.osaka-u.ac.jp.

ACKNOWLEDGMENT

We are grateful to Professor Y. Morishima at Faculty/Graduate School of Engineering, Fukui University of Technology, for fruitful discussions and valuable comments. This work was partly supported by a Grant-in-Aid for Scientific Research No. 17350058 from the Japan Society for the Promotion of Science as well as by a Grant-in-Aid for Scientific Research on Priority Area "Soft Matter Physics" and a Special Coordination Fund for Promoting Science

and Technology (Yuragi Project) of the Ministry of Education, Culture, Sports, Science and Technology, Japan.

REFERENCES

(1) Hashidzume, A.; Morishima, Y.; Szczubialka, K. In *Handbook of Polyelectrolytes and Their Applications*; Tripathy, S. K., Kumar, J., Nalwa, H. S., Eds.; American Scientific Publishers: Stevenson Ranch, CA, 2002; Vol. 2, pp 1−63.

(2) For example: (a) *Hydrophilic Polymers. Performance with Environmental Acceptability*; Glass, J. E., Ed.; Advances in Chemistry Series 248; American Chemical Society: Washington, DC, 1996. (b) *Associative Polymers in Aqueous Solutions*; Glass, J. E., Ed.; ACS Symposium Series 765; American Chemical Society: Washington, DC, 2000. (c) *Stimuli-Responsive Water Soluble and Amphiphilic Polymers*; McCormick, C. L., Ed.; ACS Symposium Series 780; American Chemical Society: Washington, DC, 2001.

(3) Kawata, T.; Hashidzume, A.; Sato, T. *Macromolecules* **2007**, *40*, 1174–1180.

(4) Tominaga, Y.; Mizuse, M.; Hashidzume, A.; Morishima, Y.; Sato, T. *J. Phys. Chem. B* **2010**, *114*, 11403–11408.

(5) (a) Tanford, C. *The Hydrophobic Effect: Formation of Micelles and Biological Membranes*, 2nd ed.; John Wiley & Sons: New York, 1980. (b) Israelachvili, J. N. *Intramolecular and Surface Forces*, 2nd ed.; Academic Press: London, 1991.

(6) (a) Borisov, O. V.; Halperin, A. *Langmuir* **1995**, *11*, 2911–2919. (b) Borisov, O. V.; Halperin, A. *Macromolecules* **1996**, *29*, 2612–2617. (c) Borisov, O. V.; Halperin, A. *Curr. Opin. Colloid Interface Sci.* **1998**, *3*, 415–421.

(7) Kikuchi, A.; Nose, T. *Macromolecules* **1996**, *29*, 6770–6777.

(8) Dubin, P.; Strauss, U. P. *J. Phys. Chem.* **1967**, *71*, 2757–2759.

(9) Dubin, P. L.; Strauss, U. P. *J. Phys. Chem.* **1970**, *74*, 2842–2847.

(10) Dubin, P.; Strauss, U. P. *J. Phys. Chem.* **1973**, *77*, 1427–1431.

(11) Strauss, U. P.; Andrechak, J. A. *J. Polym. Sci., Polym. Chem. Ed.* **1985**, *23*, 1063–1075.

(12) Binana-Limbele, W.; Zana, R. *Macromolecules* **1987**, *20*, 1331–1335.

(13) Anthony, O.; Zana, R. *Macromolecules* **1994**, *27*, 3885–3891.

(14) McCormick, C. L.; Chang, Y. *Macromolecules* **1994**, *27*, 2151–2158.

(15) Hu, Y.; Smith, G. L.; Richardson, M. F.; McCormick, C. L. *Macromolecules* **1997**, *30*, 3526–3537.

(16) Hu, Y.; Armentrout, R. S.; McCormick, C. L. *Macromolecules* **1997**, *30*, 3538–3546.

(17) Zdanowicz, V. S.; Strauss, U. P. *J. Phys. Chem. B* **1998**, *102*, 40–43.

(18) Sedimentation equilibrium and light scattering measurements were made after MAL/C12 fractions were converted to the acid form because the fractions were soluble in methanol containing 0.10 M $LiClO_4$ only in the acid form.

(19) Yamamoto, H.; Hashidzume, A.; Morishima, Y. *Polym. J. (Tokyo, Jpn.)* **2000**, *32*, 745–752.

(20) Hashidzume, A.; Kawaguchi, A.; Tagawa, A.; Hyoda, K.; Sato, T. *Macromolecules* **2006**, *39*, 1135–1143.

(21) Kanao, M.; Matsuda, Y.; Sato, T. *Macromolecules* **2003**, *36*, 2093–2102.

(22) Infelta, P. P.; Grätzel, M.; Thomas, J. K. *J. Phys. Chem.* **1974**, *78*, 190–195.

(23) Infelta, P. P. *Chem. Phys. Lett.* **1979**, *61*, 88–91.

(24) Tachiya, M. *Chem. Phys. Lett.* **1975**, *33*, 289–292.

(25) Tachiya, M. In *Kinetics of Nonhomogeneous Processes*; Freeman, G. R., Ed.; Wiley & Sons: New York, 1987; pp 575−650.

(26) The variance μ_2/Γ^2 calculated from the distribution $A(\tau)$ of the DLS relaxation time τ by

$$\mu_2/\Gamma^2 = \{\int A(\tau)\,d\tau \int \tau^{-2}A(\tau)\,d\tau/[\int \tau^{-1}A(\tau)\,d\tau]^2\} - 1$$

was ca. 0.2 for fractions MAL/C12-4−MAL/C12-7 in 0.05 M aqueous NaCl. (For the lower molecular weight fractions, μ_2/Γ^2 values calculated at different scattering angles and concentrations were so scattered that we could not determine it with a reasonable accuracy.) Using the power-law dependence $R_H \propto M^{-0.55}$ (cf. the dot-dash line in Figure 7) and the Schulz−Zimm distribution, we have $\mu_2/\Gamma^2 + 1 = \Gamma(h+2)\Gamma(h+0.9)/\Gamma^2(h+1.45)$ with $h \equiv 1/(M_w/M_n - 1)$ and the Gamma function $\Gamma(x)$. Thus, from the experimental μ_2/Γ^2, the dispersity M_w/M_n in the molar mass of the aggregates is estimated to be ca. 2.5.

(27) Kalyanasundaram, K.; Thomas, J. K. *J. Am. Chem. Soc.* **1977**, *99*, 2039–2044.

(28) Lianos, P.; Zana, R. *J. Phys. Chem.* **1980**, *84*, 3339–3341.

(29) Yashiro, J.; Hagino, R.; Sato, S.; Norisuye, T. *Polym. J. (Tokyo, Jpn.)* **2006**, *38*, 57–63.

(30) Yashiro, J.; Norisuye, T. *J. Polym. Sci., Part B: Polym. Phys.* **2002**, *40*, 2728–2735.

(31) (a) Yamada, T.; Yoshizaki, T.; Yamakawa, H. *Macromolecules* **1992**, *25*, 377–383.(b) Yamakawa, H. *Helical Wormlike Chains in Polymer Solution*; Springer: Berlin, 1997.

(32) Sato, T.; Kimura, T.; Hashidzume, A. *Prog. Theor. Phys. Suppl.* **2008**, *175*, 54–63.

(33) The inverse proportionality of m_w to the degree of polymerization of an associating polymer was derived theoretically by Potemkin et al.[40] and supported by experiment on chitosan in dilute aqueous solution of Korchagina and Philippova.[41] However, Potemkin et al.'s polymer aggregate ("cluster") model is not the unicore flower micelle, but a random aggregate where polymer chains form a network and the associating group ("sticker") has no specific optimum aggregation number. Therefore, the inverse proportionalities of m_w to N_{w1} they predicted and our finding for the unicore flower micelle arise from different origins.

(34) Flory, P. J. *Statistical Mechanics of Chain Molecules*; John Wiley & Sons: New York, 1969.

(35) Sato, T.; Terao, K.; Teramoto, A.; Fujiki, M. *Polymer* **2003**, *44*, 5477–5495.

(36) (a) Odijk, T. *J. Polym. Sci., Polym. Phys. Ed.* **1977**, *15*, 477–483. (b) Odijk, T. *Polymer* **1978**, *19*, 989–990.

(37) Skolnick, J.; Fixman, M. *Macromolecules* **1977**, *10*, 944–948.

(38) Douglas, J. F.; Roovers, J.; Freed, K. F. *Macromolecules* **1990**, *23*, 4168–4180.

(39) Kajiwara, K.; Ribeiro, C. A. M. *Macromolecules* **1974**, *7*, 121–128.

(40) Potemkin, I. I.; Andreenko, S. A.; Khokhlov, A. R. *J. Chem. Phys.* **2001**, *115*, 4862–4872.

(41) Korchagina, E. V.; Philippova, O. E. *Biomacromolecules* **2010**, *11*, 3457–3466.